Development 126, 3585-3596 (1999)
Printed in Great Britain © The Company of Biologists Limited 1999
DEV1435

Role of *Pax6* in development of the cerebellar system

Dieter Engelkamp*, Penny Rashbass‡, Anne Seawright and Veronica van Heyningen§

MRC Human Genetics Unit, Western General Hospital, Crewe Road, Edinburgh, EH4 2XU, Scotland
*Present address: Max Planck Institut für Hirnforschung, Deutschordenstrasse, 46, 60528 Frankfurt, Germany
‡Present address: Developmental Genetics Programme, University of Sheffield, Firth Court, Western Bank, Sheffield S10 2TN, UK
§Author for correspondence (e-mail: v.vanheyningen@hgu.mrc.ac.uk)

Accepted 4 June; published on WWW 19 July 1999

SUMMARY

Post-mitotic neurons generated at the rhombic lip undertake long distance migration to widely dispersed destinations, giving rise to cerebellar granule cells and the precerebellar nuclei. Here we show that *Pax6*, a key regulator in CNS and eye development, is strongly expressed in rhombic lip and in cells migrating away from it. Development of some structures derived from these cells is severely affected in *Pax6*-null Small eye (*Pax6^{Sey}/Pax6^{Sey}*) embryos. Cell proliferation and initial differentiation seem unaffected, but cell migration and neurite extension are disrupted in mutant embryos. Three of the five precerebellar nuclei fail to form correctly. In the cerebellum the pre-migratory granule cell sub-layer and fissures are absent. Some granule cells are found in ectopic positions in the inferior colliculus which may result from the complete absence of *Unc5h3* expression in *Pax6^{Sey}/Pax6^{Sey}* granule cells. Our results suggest that *Pax6* plays a strong role during hindbrain migration processes and at least part of its activity is mediated through regulation of the netrin receptor *Unc5h3*.

Key words: *Small eye*, Rhombic lip, Precerebellar nuclei, Neural cell migration, Netrin receptors, Mouse

INTRODUCTION

The cerebellum is one of the best studied regions of the central nervous system. Important functional information about its development has already been gained through analysis of neurological mutants (Hatten and Heintz, 1995). Here we assess the role of the *Pax6* gene in development of cerebellar structures, by comparing normal and *Pax6*-mutant Small eye mice at different gestational stages.

The role of *Pax6* in eye development has been the major focus of attention (Hanson and van Heyningen, 1995; Callaerts et al., 1997). *Pax6* misexpression experiments resulting in ectopic eye development from *Drosophila* leg, wing and antennal discs, led to suggestions that *Pax6* is a master control gene for eye development (Halder et al., 1995). However, the broader *Pax6* expression pattern in brain, neural tube and nasal placodes, and the presence and function of the gene in *C. elegans* (Chisholm and Horvitz, 1995; Zhang and Emmons, 1995) suggest a more general ancestral role in sensorineural development. Severe CNS abnormalities observed in homozygous *Pax6^{Sey}/Pax6^{Sey}* mice include defects in forebrain patterning (Grindley et al., 1997; Stoykova et al., 1996; Warren and Price, 1997), axonal pathfinding (Mastick et al., 1997), and motor neuron and glial cell subtype specification (Ericson et al., 1997; Götz et al., 1998; Osumi et al., 1997; Sun et al., 1998). A role in cortical neuronal migration has also been suggested (Caric et al., 1997; Schmahl et al., 1993), but this has been difficult to analyse, as these anomalies are superimposed on earlier patterning abnormalities caused by the *Pax6* mutation.

In this study we examine the role of *Pax6* in the development of rhombic lip derivatives, since a high proportion of cells in the precerebellar neuroepithelium and the developing cerebellum are *Pax6*-expressing but the cerebellum is retained in *Pax6^{Sey}/Pax6^{Sey}* embryos as a readily recognisable, though morphologically altered, structure. *Pax6^{Sey}/Pax6^{Sey}* embryos die at birth, but early development of cerebellar structures can be studied up to E19 in *Pax6*-null embryos.

Using specific antibodies and in situ hybridisation, we studied rhombic lip-derived neuronal populations. Our results suggest that *Pax6* plays a key role in defining the identity of a subset of precerebellar and cerebellar neurons and their ability to reach their target sites in *Pax6^{Sey}/Pax6^{Sey}* mice.

The cerebellum develops as part of the rhombencephalon at a region of incomplete closure of the dorsal neural tube. The rim of the 'open' neural tube is often referred to as the rhombic lip. Upper (rostral) and lower (caudal) lips are brought into close apposition when the pontine flexure develops. The rostral lip gives rise only to cerebellar granule cell precursors (Alder et al., 1996; Hallonet et al., 1990; Zhang and Goldman, 1996). The caudal lip undergoes a series of morphological transformations to form the highly proliferative precerebellar neuroepithelium (pcn) (Altman and Bayer, 1987) in the dorsal medulla. Neurons generated by the pcn migrate out sequentially, along divergent pathways, to form the precerebellar nuclei, all of which project to the cerebellum

(Altman and Bayer, 1987; Essik, 1912; His, 1891). These nuclei come to lie in the pontine and medullary regions of the hindbrain. The five pre-cerebellar nuclei are: the inferior olive, the external cuneate and lateral reticular nuclei in the medulla and the pontine and reticulotegmental nuclei in the pons (Altman and Bayer, 1987). Three distinct migration streams carry cells from the pcn to the five nuclei. Cells of the anterior extramural stream (aes) cross several rhombomere boundaries (Marín and Puelles, 1995) before settling ipsilaterally in the pontine and reticulotegmental nuclei. Cells in the posterior extramural stream (pes) cross the midline and settle contralaterally in the lateral reticular and external cuneate nuclei in the medulla (Altman and Bayer, 1987). The aes and pes encircle the hindbrain using pathways perpendicular to the glial fibres which radiate across the medulla. The inferior olive, in contrast, is populated by cells using a third, intramural, migration path. Formation of the pontine, external cuneate and lateral reticular nuclei is disrupted in *Pax6^{Sey}/Pax6^{Sey}* mice.

Signals required to accomplish these migrations are beginning to be defined. Genetic ablation experiments suggest that secreted netrins and their receptors play a role not only in axonal pathfinding, but also in neuronal migration (Ackerman et al., 1997; Fazeli et al., 1997; Serafini et al., 1996). The secreted molecule Netrin 1 (Ntn1) is expressed in the floor plate of the vertebrate neural tube (Kennedy et al., 1994) and may serve as an attractive signal to migrating precerebellar neurons. Two classes of receptors have been defined: the *Dcc* ('deleted in colon cancer') family and the *Unc5* (homologues of the *C elegans* un-coordinated *unc5* gene) family Interestingly, in mice homozygous for knock-out of either *Ntn1* (Serafini et al., 1996) or its receptor *Dcc* (Fazeli et al., 1997) the pontine nuclei are also absent. Cerebellar granule cell progenitors originate in the rostral rhombic lip, from embryonic day 13 (E13) in the mouse. Cells undergo three successive modes of migration, each perpendicular to the others. Initial movement is by proliferating neurons in a rostral direction, along the surface of the cerebellar primordium, to form the external granular layer (EGL) of the cerebellum (Hatten and Heintz, 1995; Ramón y Cajal, 1995). By E16 the whole cerebellar surface is covered with a thin layer of granule cells (Miale and Sidman, 1961), which, in the chick, have been shown move transversely, in both medial to lateral and lateral to medial directions, with the latter predominating (Hallonet et al., 1990; Ryder and Cepko, 1994). The rostral and lateral migrations are not along radial glial fibres. The final migration, between the first and third postnatal weeks, is inward, along radial glial fibres, to form the internal granular layer of the cerebellum (Hatten and Heintz, 1995; Rakic, 1990).

Markers used to assess EGL cell identity include the developmental regulators *Math1*, an atonal-like bHLH transcription factor, and *Zic1* and *Zic2*, two related zinc finger genes. Mouse knockouts for *Math1* revealed it to be essential for cerebellar granule cell development (Ben-Arie et al., 1997), while *Zic1* targeted deletions lead to defects in cerebellar cell proliferation and foliation (Aruga et al., 1998). Heterozygous mutations in human *ZIC2* have been associated with holoprosencephaly (Brown et al., 1998).

Loss of functional Pax6 protein in *Pax6^{Sey}/Pax6^{Sey}* EGL cells does not alter the expression of several granule cell specific markers, but expression of *Unc5h3*, the netrin receptor gene mutated in the *rcm* (rostral cerebellar malformation) mouse (Ackerman et al., 1997; Przyborski et al., 1998), is abolished in these cells. Neighbouring Purkinje cells, derived from different progenitors, continue to express Unc5H3. As the mutant granule cells mature and become post-mitotic they fail to organise themselves normally. The mutant EGL layer is broadened and no cerebellar fissures are formed, perhaps as a result of aberrant migration. Cerebellar explant cultures reveal alterations in neurite outgrowth and the migratory behaviour of *Pax6^{Sey}/Pax6^{Sey}*-derived neurons.

MATERIALS AND METHODS

Animals

All mouse embryos were derived from *Pax6^{Sey}/+* × *Pax6^{Sey}/+* crosses (Roberts, 1967) on an outbred Swiss or an inbred CBA background. E0.5 denotes the morning when the copulation plug was found. Littermates were always used for comparisons between wild-type and *Pax6^{Sey}/Pax6^{Sey}* The mutation in *Pax6^{Sey}* is G194X, predicted to result in a truncated protein lacking the homeodomain and C-terminal sequences (Hill et al., 1991). All phenotypes described were confirmed in a second allelic *Pax6* mutant, *Pax6$^{Sey\text{-}Neu}$* (Hill et al., 1991).

Production of Pax6-specific monoclonal antibodies and western blots

The N-terminal 206 amino acids of human PAX6, fused in frame to a C-terminal 6xHis-Tag, were expressed in a bacterial expression system (PET11, Novagen) and BALB/c mice were injected intraperitoneally with 25 μg of purified protein (in Hunter's TiterMax, Sigma). Two more injections, each with 10 μg of the protein, were given 4 and 2 days prior to fusion. Spleen cells were fused with Sp2/0 myeloma cells using the method of Köhler and Milstein (Köhler and Milstein, 1975). Supernatants from individual hybridoma clones were initially screened by ELISA using the immunogen as antigen. Positive clones were analysed for cross-reactivity with other members of the Pax gene family by screening COS cells transfected with expression constructs of individual full length Pax cDNAs (*Pax2, 5, 6, 7, 8*). Further tests included staining of primary cells derived from Pax6+ or Pax6− tissues. Clones selectively recognising Pax6 (AD1.5, AD2.3, AD2.35, and AD2.38) were grown in the MiniPerm system (Heraeus) to produce concentrated culture supernatants. Western Blots were performed as described in Larsson et al. (Larsson et al., 1995).

Immunohistochemistry

The monoclonal antibody, MEN-B, against PSA-NCAM (polysialylated neural cell adhesion molecule) (1:500) and the rabbit anti-NCAM (1:100) were a generous gift from G. Rougon (Rougon et al., 1986). Rabbit anti-tau (microtubule associated neurofibrillary protein) (1:100), monoclonal anti-Calbindin D28K (1:2000), anti-GAP-43 (1:100) were from Sigma; rabbit anti-GFAP (1:100) was from DAKO; rabbit anti-Pax2 was from G. Dressler (Dressler and Douglass, 1992) (it should be noted, however, that the peptide against which this antibody was raised is highly conserved between Pax2, 5 and 8 and the antibody may recognise all three); monoclonal anti-Dcc (Deleted in Colorectal Cancer – a netrin receptor) from Calbiochem; monoclonal 3CB2 (recognising radial glial fibres) (1:50; Prada et al., 1995) and RC2 (recognising radial glial fibres) (1:100; Misson et al., 1988) were from the Developmental Studies Hybridoma Bank and grown in the MiniPerm system (Heraeus); monoclonal TuJ1 (directed against neural-specific beta tubulin (1:500) was from A. Frankfurter and from BAbCo (Lee et al., 1990). Second antibodies and conjugates were from Jackson Immunolabs (used at 1:500). For most applications, dissected brains were fixed in 1% paraformaldehyde/1% sulfosalicylic acid (Sigma; w/v, in PBS), embedded in paraffin wax and 6 μm serial sections were cut. RC2 staining was on 75-150 μm vibratome sections

of brains fixed in 2% paraformaldehyde. Dcc staining was on cryostat sections of brains fixed with 4% paraformaldehyde. Sections were successively incubated with primary antibody, biotinylated second antibody and with peroxidase-conjugated streptavidin. Staining was visualised with DAB using the metal-enhancement method (Sigma). Pax6 expression pattern was confirmed using individual anti-Pax6 monoclonal antibodies, but for illustration purposes images of paraffin embedded sections were obtained using a 1:1 mixture of AD2.35 and AD2.38 (1:50) and images of cerebellar cultures were obtained using AD1.5 (1:50). Images were taken on a Zeiss Axioplan 2 and on a Leica MZ12 microscope.

BrdU labelling and apoptosis

Bromodeoxyuridine (BrdU; Boehringer; 50 mg/kg body weight in PBS) was injected into pregnant dams 1 hour before killing them. In some experiments BrdU injection was 24, 72, 96 or 120 hours before death. In the cumulative labelling experiment mice were injected 6 times over a period of 15 hours. To follow the pontine migrations mice were injected four times between E13.5 and E14.5 and then killed at E18.5. The embryonic stages at which experiments were performed are described under Results. Brain sections were successively incubated with 0.1% trypsin/0.1% $CaCl_2$ in PBS for 10 minutes at 37°C and with 4 N HCl for 10 minutes at RT, stained with monoclonal anti-BrdU antibody (Becton Dickinson) as described above and lightly counter-stained with methyl green. Apoptotic cells were detected by TUNEL assay (Boehringer).

Cerebellar microexplant cultures

Microexplant cultures were set up as described by Nakatsuji and Nagata (1989), with minor modifications. Wild-type and *Pax6^{Sey}/Pax6^{Sey}* cerebella were dissected at E17.5 or E18.5 and strips of external granular layer were removed using a razor blade under a dissecting microscope. The EGL strips were further cut into small pieces (∅ <0.5 mm) and cultured in glass chamber slides (Nunc) coated with 100 μg/ml poly(L)-lysine (Sigma) and 100 μg/ml laminin (Sigma). Serum-free medium used was: DMEM (49.5%), F10 medium (49.5%) and 1% N1 supplement (Sigma; 5 μg/ml insulin; 5 μg/ml transferrin; 20 nM progesterone; 100 μM putrescine; 30 nM selenium). Explants were cultured at 37°C in 5% CO_2 and analysed after 17, 40 or 72 hours in culture. Microexplant cultures were fixed in methanol:acetone (1:1, −20°C), rehydrated in PBS and successively incubated with primary and FITC- or TRITC-conjugated second antibodies. Images were taken on a Zeiss Axioplan microscope using a digital imaging system.

Non-radioactive RNA in situ hybridisation

Digoxigenin (DIG)-labelled anti-sense riboprobes were synthesised according to the manufacturers protocol (Boehringer Mannheim). In situ hybridisation of frozen sections was as described by Strähle et al. (1994). For whole-mount preparations embryos were dissected, fixed overnight in 4% paraformaldehyde/PBS, transferred stepwise to 100% methanol and stored at −20°C. Tissue was rehydrated to PBS, bleached with 6% H_2O_2 in PBT (PBS, 0.1% Tween-20) for 4 hours, proteinase K (10 μg/ml) digested for 15 minutes and pre-hybridised overnight (in hybridisation solution plus 2% Boehringer blocking reagent). For hybridising, washing (1× SSC/50% formamide followed by 0.2× SSC/50% formamide) and DIG visualisation, essentially the same procedure was used as for the sectioned material albeit at extended incubation times. Some whole-mount preparations were sectioned subsequently to reveal internal marker expression.

Probes were received as follows: mouse *Math1* from H. Y. Zoghby (Ben-Arie et al., 1997), *Zic1* and *Zic2* from J. Aruga (Aruga et al., 1998), *Unc5h3* (rcm) from S. Ackerman (Ackerman et al., 1997), *Pax6* from R. E. Hill (Grindley et al., 1995) and *Ntn1* and rat *Dcc* from M. Tessier-Lavigne (Keino-Masu et al., 1996; Serafini et al., 1996).

RESULTS

Production of Pax6-specific monoclonal antibodies

Four Pax6-specific monoclonal antibodies were generated against a Pax6 protein fragment corresponding to the first 206 amino acids (Fig. 1A). Antibody specificity was assessed using a number of different assays (see Materials and Methods) which permitted assignment of approximate epitope positions (Fig. 1A). On western blotting each antibody recognises the expected 46 and 48 kDa Pax6 proteins (Fig. 1B) representing products of the two major alternatively spliced *Pax6* mRNAs (–/+ exon 5a). The ratio of the two isoforms (approximately 5:1, −5a:+5a) was found to be identical at all developmental stages and in all tissues examined (data not shown). All four antibodies recognise human, mouse, rat and chick Pax6 and two (AD1.5 and AD2.3) also react with the zebrafish protein (data not shown). Immunohistochemistry using individual antibodies on mouse, rat and chick embryo sections demonstrated that the protein pattern is similar to the published transcript distribution (Grindley et al., 1995; Stoykova and Gruss, 1994; Walther and Gruss, 1991).

Antibodies AD2.38 and AD2.35, used together in immunohistochemistry, recognise the truncated Pax6 protein fragment expected in *Pax6^{Sey}/Pax6^{Sey}* mice, although expression level is much reduced, and sometimes undetectable in cells where the presence of transcripts is demonstrable by RNA in situ analysis.

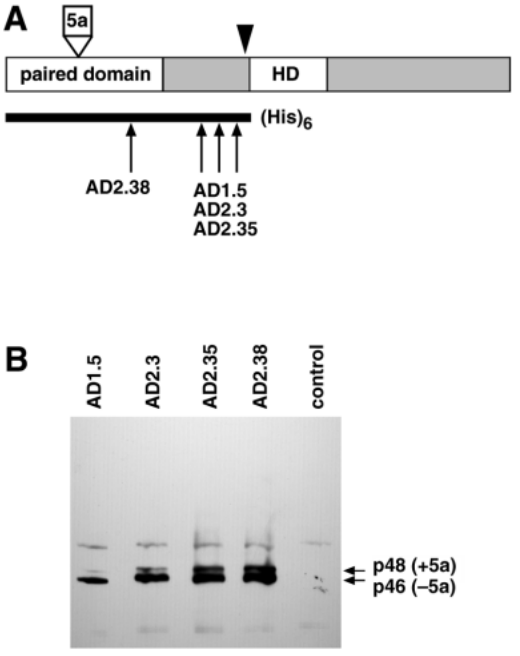

Fig. 1. Pax6 specific monoclonal antibodies. (A) Schematic of the two major Pax6 proteins generated by alternative splicing of exon 5a. Approximate positions of epitopes recognised by individual monoclonal antibodies are indicated by arrows. HD marks the homeodomain; the black bar represents the bacterially expressed N-terminal domain of Pax6 used as antigen; the arrowhead indicates position of *Pax6^{Sey}* mutation. (B) Western blot of Pax6 protein, demonstrating specifity of individual antibodies. Each lane contains nuclear extracts of 4 P1 mouse cerebella.

Requirement for PAX6 during development of the precerebellar nuclei

Whole-mount RNA in situ hybridisation and antibody staining show Pax6 to be highly expressed at E12.5, and subsequently throughout the period of active neurogenesis, in the rhombic lip of wild-type mice (Fig. 2A,B). Strong Pax6 expression is detected at E16.5 in the pcn (Fig. 2C), and in two of the three migration streams extending from it: the aes (Fig. 2D) and the pes (data not shown). In wild-type brain, aes cells are strongly Pax6+ during migration and as they reach their target sites, but subsequently expression levels decline gradually (Fig. 2D). In *Pax6^{Sey}/Pax6^{Sey}* embryos the aes and pontine nuclei are much reduced (Fig. 2E).

The role of likely guidance molecules was assessed. PSA-NCAM levels are low (Fig. 2F) in the Pax6+ migrating cells of the aes (Fig. 2G), but the aes boundaries, formed by Pax6– cells, express high levels of PSA-NCAM (compare Fig. 2F and 2G). PSA-NCAM-expressing boundary cells are maintained in *Pax6^{Sey}/Pax6^{Sey}* embryos (Fig. 2H), although the Pax6+ aes is absent, suggesting that the migratory paths are determined by mechanisms independent of *Pax6* expression. Both the aes and pes tracts are negative for radial glial markers RC2 (Misson et al., 1988) (Fig. 2I) and 3CB2 (Prada et al., 1995) (data not shown).

Altered precerebellar migrations in *Pax6^{Sey}/Pax6^{Sey}* embryos

Cell numbers in the *Pax6^{Sey}/Pax6^{Sey}* aes and pontine nucleus were estimated to be reduced to less than 10% of wild-type, by

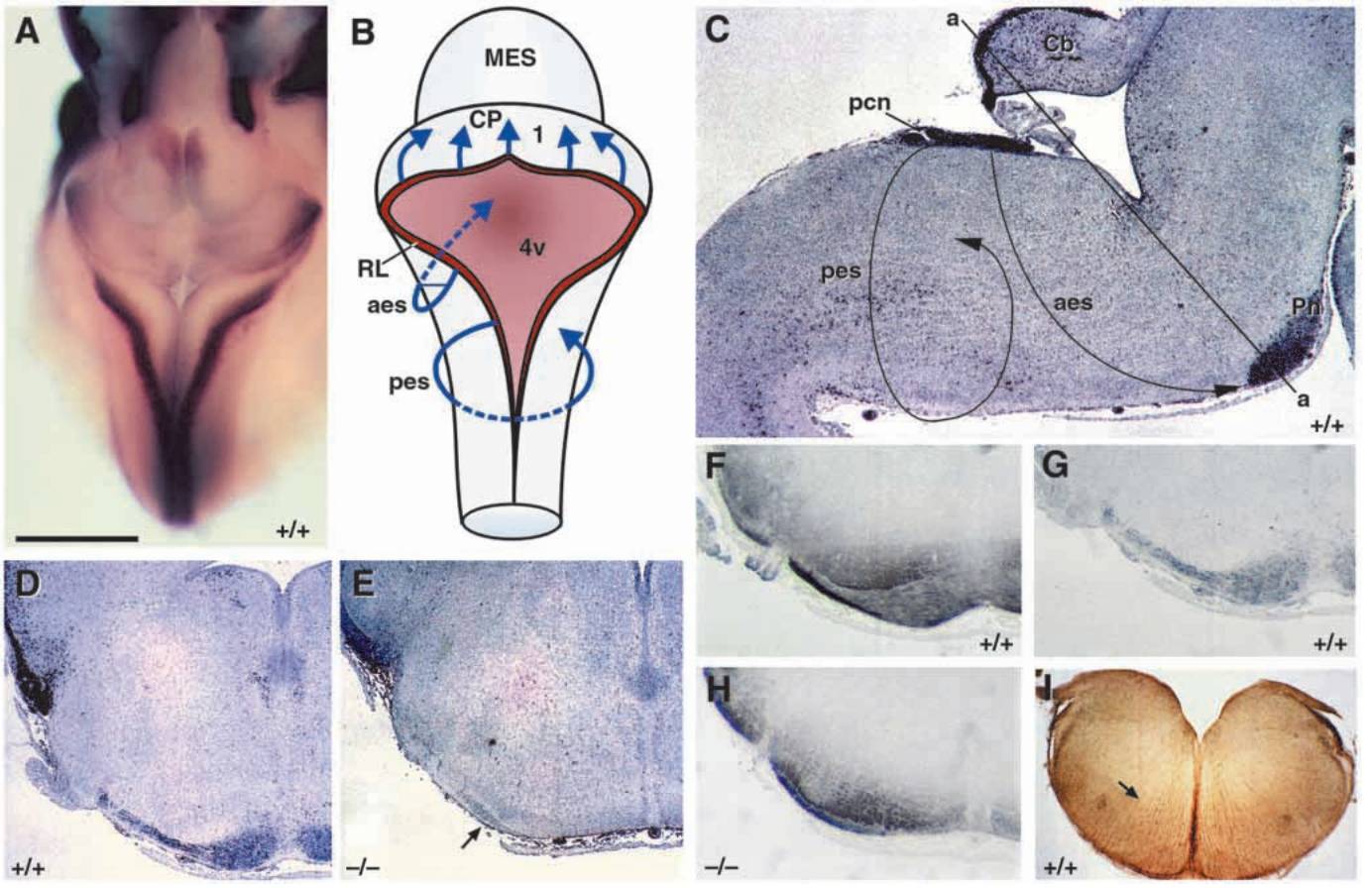

Fig. 2. Migration streams from the precerebellar neuroepithelium (i). (A) Whole-mount Pax6 in situ hybridisation of E12.5 embryo. Dorsal side of embryo is shown with rostral up. The mesencephalon was partially removed to reveal the cerebellar primordium. Strong Pax6 expression is seen in the lower rhombic lip. Pax6 expression in the upper rhombic lip reaches comparable levels by E13.5 (not shown). (B) Schematic of the hindbrain region shown in A, indicating migration directions taken by neurons derived from the rhombic lip. Neurons derived from the lower rhombic lip migrate ventrally along the anterior and posterior migration streams, whereas neurons derived from the rostral rhombic lip migrate dorsally (1) to cover the cerebellar primordium. (C) Parasagittal section through the caudal region of wild-type E16.5 brain showing Pax6 protein expression domains in the cerebellum, the precerebellar neuroepithelium and pontine nucleus. Anterior is right. Curved arrows indicate route taken by precerebellar neurons. Line 'a' indicates planes of section forD to I. (D) Wild-type and (E) *Pax6^{Sey}/Pax6^{Sey}* E16.5 brain stained with anti-Pax6 antibody showing reduction of the aes to a few cells (E, arrow). (F,G) Consecutive wild-type E16.5 coronal sections stained for PSA-NCAM (F) and Pax6 (G). Strongly PSA-NCAM-positive fibres form the outer margins of the aes. Weak PSA-NCAM staining is seen in the region of Pax6+ migrating cells. (H) *Pax6^{Sey}/Pax6^{Sey}* E16.5 coronal section matched to wild-type sections (F) and (G) stained for PSA-NCAM. The remaining aes is still bordered by strongly PSA-NCAM positive fibres. (I) Coronal vibratome section of E16.5 wild-type hindbrain: RC2 positive glial cells are radial (arrow), perpendicular to the orientation of *Pax6* positive migrations (compare Fig. 2D). aes, anterior extramural migration stream; Cb, cerebellum; CP, cerebellar primordium; MES, mesencephalon; pes, posterior extramural migration stream; pcn, precerebellar neuroepithelium; Pn, pontine nuclei; RL, rhombic lip; 4v, fourth ventricle; +/+ and –/– indicate wild-type and *Pax6^{Sey}/Pax6^{Sey}* embryos respectively. Scale bar, 1 mm in A, I; 500 μm in C-H.

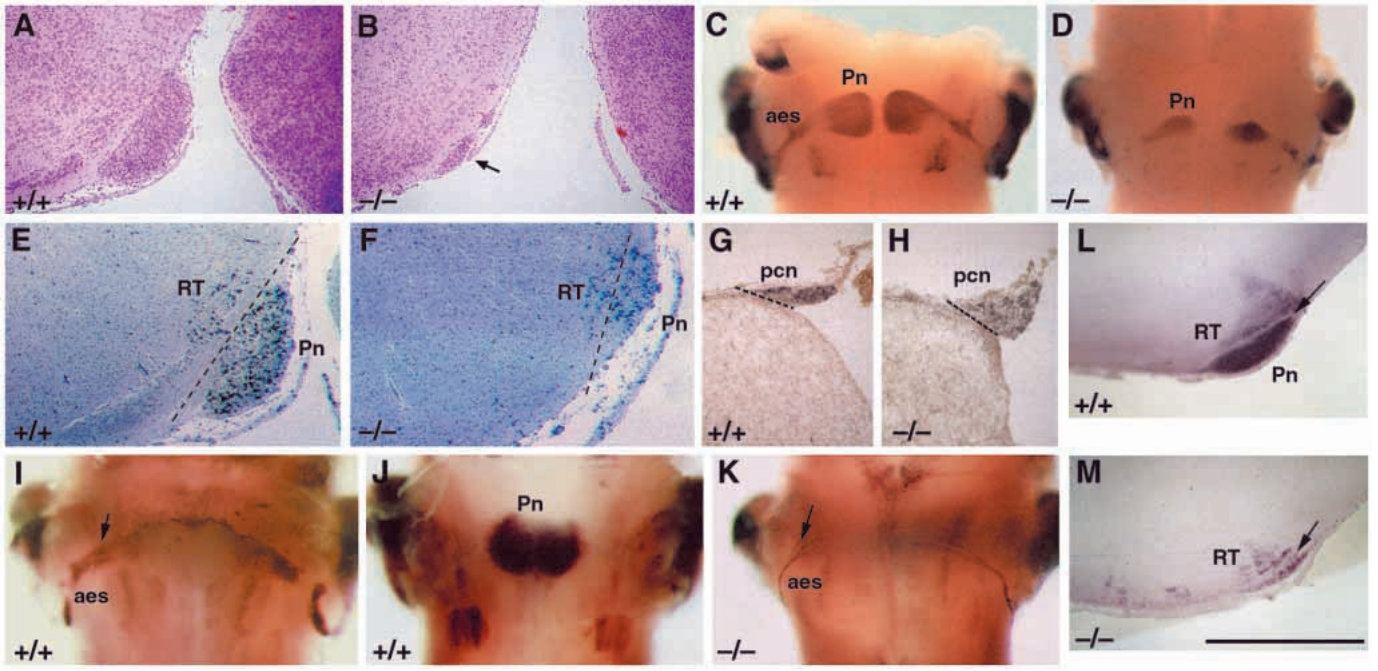

Fig. 3. Migration streams from the precerebellar neuroepithelium (ii). (A) Wild-type and (B) *Pax6^{Sey}/Pax6^{Sey}* H+E stained parasagittal sections of E19.5 pons show almost complete absence of pontine nuclei in *Pax6^{Sey}/Pax6^{Sey}* embryos (arrow). Anterior is right. (C) Wild-type and (D) *Pax6^{Sey}/Pax6^{Sey}* E18.5 embryos showing Pax6 expression by whole mount in situ hybridisation. Ventral side is shown with rostral up. There is a strong reduction of aes and pontine nuclei in the *Pax6^{Sey}/Pax6^{Sey}* embryo. Preliminary studies suggest that the small caudal patches of Pax6 expression in wild-type are in the superior olivary nuclear complex. (E,F) Parasagittal sections of (E) wild-type and (F) mutant E18.5 pons stained with BrdU. Anterior is right. Dividing neurons were cumulatively labelled with BrdU between E13.5 and E14.75. The majority of neurons in the pontine nuclei are positive for BrdU indicating that they were generated between E13.5 and E14.75. The pontine reticulotegmental nucleus is apparently unaltered in *Pax6^{Sey}/Pax6^{Sey}* embryos. Dashed line indicates Pn/RT boundary. (G) Wild-type and (H) *Pax6^{Sey}/Pax6^{Sey}* coronal sections at E16.5 stained for Pax6 by in situ hybridisation: the precerebellar neuroepithelium (outlined by dotted line) is enlarged in the mutant. Ventral is down and medial right. (I-K) Whole-mount RNA in situ hybridisation of wild-type (I,J) and mutant (K) E16.5 hindbrain with Dcc (I,K) and Unc5h3 (J) as probes. Ventral side is shown with rostral pointing up. Dcc is expressed only in actively migrating neurons in the aes. Unc5h3 is only expressed in neurons settling in the pontine nuclei and not in the aes The remaining aes neurons in the mutant still express Dcc (K). (L,M) Parasagittal vibratome sections of whole-mount RNA in situ hybridisation with Unc5h3 of wild-type (L) and mutant (M) E18.5 hindbrain. Anterior is right. Unc5h3 labels both the pontine and the reticulotegmental nuclei, which are separated by the corticospinal tract (arrowed). In the mutant the reticulotegmental nucleus is unaltered whereas the pontine nucleus is much reduced. aes, anterior extramural migration stream; pcn, precerebellar neuroepithelium; Pn, pontine nuclei; RT, reticulotegmental nuclei; +/+ and –/– indicate wild-type and *Pax6^{Sey}/Pax6^{Sey}* embryos respectively. Scale bar, 400 μm in A,B,E,F; 1.6 mm in C,D,I,J,K; 300 μm in G,H; 600 μm in L,M.

counting H&E stained cells (see Fig. 3A,B) and by tissue volume analysis using camera lucida drawings of serial sections. The pes and the *Pax6*+ cells it normally conveys to the lateral reticular and external cuneate nuclei are severely disorganised in *Pax6^{Sey}/Pax6^{Sey}* brain (D. E. et al., unpublished data). Reduction in the *Pax6*+ aes and its target nuclei is illustrated (Fig. 3C,D). Possible causes for the loss of migration streams and precerebellar nuclei are: changes in cell proliferation, cell death, or aberrant migration. These parameters were examined in wild-type and mutant mice.

Cell proliferation was studied by analysing BrdU incorporation into S-phase cells and visualisation using anti-BrdU antibody (Takahashi et al., 1992). Mitotically active zones are defined by analysis soon after labelling. Cell migration is followed by studying cell number and position at defined times following BrdU application. To identify the embryonic stage at which the neurons of the pontine nuclei are generated, a single dose of BrdU was applied at three different developmental stages: E13.5, E14.5 and E15.5. Embryos were then allowed to develop to E18.5, collected, fixed, and the number of BrdU-positive (BrdU+) and BrdU-negative (BrdU–) nuclei determined on sagittal sections of the pontine region. Embryos injected at E13.5 had 46% labelled pontine cells, while those injected at E14.5 and E15.5 only had 17% and 9% respectively. Four cumulative injections between E13.5 and E14.5, followed by embryo collection at E18.5, produced 62% BrdU+ pontine cells (data not shown and Fig. 3E). In agreement with previous studies in rat and mouse (Altman and Bayer, 1987; Pierce, 1966), the majority of neurons destined for the pontine are therefore generated between E13.5 and E14.5. The cumulative number and volume of labelled cells arriving at the *Pax6^{Sey}/Pax6^{Sey}* pontine region is much reduced, although the reticulotegmental nuclei are formed normally (Fig. 3E,F), suggesting that the aes pathway itself is not affected by the mutation.

Proliferative activity of the pcn during neurogenesis was assessed by BrdU incorporation following 1 hour exposure at E13.5. Identical areas of the pcn, delineated by camera lucida drawings of alternate BrdU- and Pax6-stained sections, were studied in wild-type and in *Pax6^{Sey}/Pax6^{Sey}* embryos, showing

35.1% (±1.3) (*n*=3; mean number BrdU+ cells: 3436; mean number BrdU– cells: 6755) and 35.8% (±2.4) (*n*=3; mean number BrdU+ cells: 3100; mean number BrdU– cells: 5397) proliferating cells respectively. This suggests unaltered proliferation in mutant mice. Similarly, no differences in proliferative capacity were found with injection at E14.5 or E15.5. Neurons of the pcn, destined for the precerebellar nuclei are therefore generated at a normal rate in *Pax6^{Sey}/Pax6^{Sey}* embryos.

Using the TUNEL assay, no increase was detected in the very low levels (approx. 1%) of apoptosis observed in E13.5, E14.5, E15.5 or E16.5 embryos (data not shown). However, at E16.5 the pcn is enlarged in *Pax6^{Sey}/Pax6^{Sey}* embryos (compare Fig. 3G and 3H), suggesting that cells which express no functional Pax6 protein can proliferate and survive normally, but accumulate abnormally at the site of cell generation, apparently unable to migrate via the aes and pes to their target sites. In contrast, the inferior olive, arising early from pcn-derived cells (Altman and Bayer, 1987) which are Pax6–, forms normally in *Pax6^{Sey}/Pax6^{Sey}* embryos.

Neuronal marker analysis to search for alteration in cell identity

To define possible changes in cell identity which might interfere with migration of pcn cells to their target sites, we examined the expression of the netrin receptors Dcc and Unc5h3 in precerebellar neurons. In wild-type embryos whole-mount in situ hybridisation reveals Dcc expression only in actively migrating neurons in the aes (Fig. 3I). Dcc is absent from proliferating pcn neurons (not shown) and from neurons arriving at the pontine nuclei (Fig. 3I). In contrast, Unc5h3 is expressed by neurons only as they arrive at the pontine nuclei (Fig. 3J), but absent from the pcn and aes. In the *Pax6^{Sey}/Pax6^{Sey}* mutant, Dcc is still expressed in the few remaining migrating cells of the aes (Fig. 3K), suggesting that Ntn1/Dcc interactions are not disturbed by the mutation. At E18.5 a few residual Unc5h3-expressing cells are found in the *Pax6^{Sey}/Pax6^{Sey}* pontine remnants, although expression in the neighbouring reticulotegmental nuclei is unaffected (Fig. 3L,M). Ntn1 expression is unaltered in *Pax6^{Sey}/Pax6^{Sey}* embryos (data not shown).

Developmental changes in *Pax6^{Sey}/Pax6^{Sey}* cerebellum

Changes in gross structure and foliation

Wild-type cerebellum at E18.5 has an almost uniform rostro-caudal width across its entire breadth (Fig. 4A) and by E19.5 five to six lobes have formed, separated by deep fissures (Fig. 4B). In contrast, the *Pax6^{Sey}/Pax6^{Sey}* cerebellum bulges at the lateral edges, and has a narrowed central vermal region (Fig. 4A). It fails to form any fissures (Fig. 4C).

In E15.5 *Pax6^{Sey}/Pax6^{Sey}* embryos the EGL forms apparently normally, showing only slight delay in covering the most mediorostral aspect of the cerebellar primordium. Differences between wild-type and *Pax6^{Sey}/Pax6^{Sey}* cerebellar development become more apparent between E17.5 and E19.5.

Cell proliferation is unaffected

The *Pax6^{Sey}/Pax6^{Sey}* cerebellar phenotype could be caused by a defect in either granule cell proliferation or migration. Both were assessed. The total number of wild-type and mutant granule cells at E18.5 was estimated. Paraffin sections from E18.5 wild-type and *Pax6^{Sey}/Pax6^{Sey}* littermates were processed and sectioned simultaneously, and H+E stained granule cells were counted on photographic prints taken from every tenth section. Total counts (35,298 in wild-type; 30,000 in mutants) were corrected for differences in cell density (*Pax6^{Sey}/Pax6^{Sey}* granule cells are 6.5% more densely packed than wild-type cells) and integrated over the total number of cerebellar sections (13 each). The total number of wild-type granule cells is estimated to be 1.9% higher than the total number of mutant granule cells. This difference is well within the estimated counting error of 5%.

To investigate mitotic rates, proliferating granule cells were labelled with BrdU at E15.5 or at E18.5 and labelling indices (LI = ratio of BrdU positive to total cells) determined. No significant differences in LI between wild-type and mutant EGL were found (Table 1 and data not shown). Therefore, no proliferation defect in the *Pax6^{Sey}/Pax6^{Sey}* EGL is observed prior to or at E18.5.

Organisation of post-mitotic granule cells is disturbed

Simple visual inspection of H+E-stained histological sections reveals altered organisation in *Pax6^{Sey}/Pax6^{Sey}*. At E19.5 the EGL layer appears broader in mutant mice, and there is an absence of fissure formation (Fig. 4B,C). At E18.5 granule cell bodies in the premigratory zone of wild-type EGL are elongated parallel to the cerebellar surface in a lateral to medial orientation (Fig. 4D,E), while in *Pax6^{Sey}/Pax6^{Sey}* embryos, there is failure to reorient or move away from the germinal layers into a distinct pre-migratory layer (Fig. 4F).

Granule cell commitment to neuronal cell fate and the ability

Table 1. Determination of cerebellar granule cell proliferation

	Embryo ID	Lateral				Semi-medial				Medial				
		BrdU+	Total	LI	*n*	BrdU+	total	LI	*n*	BrdU+	total	LI	*n*	average LI
wild-type	#1	541	1757	30.8	6	475	1530	31.0	5	373	1072	34.8	4	**31.9**
	#2	695	2029	34.3	7	597	2093	28.5	6	458	1144	40.0	4	**33.2**
	#3	656	1969	33.3	6	470	1195	39.3	5	358	1018	35.2	5	**35.6**
	sum			**32.8**				**32.9**				**36.7**		**33.5±1.1**
Pax6^{Sey}/Pax6^{Sey}	#4	947	2411	39.3	6	540	1553	34.8	4	579	1572	36.8	4	**37.3**
	#5	1279	3300	38.8	7	807	2397	33.7	6	627	1708	36.7	4	**36.6**
	#6	697	2159	32.3	5	680	1868	36.4	5	561	1441	38.9	5	**35.4**
	sum			**36.8**				**35.0**				**37.5**		**36.5±1.5**

Labelling indices (LI: percentage of BrdU-positive versus total number of cells) of the E18.5 EGL was determined in 3 wild-type and 3 mutant embryos derived from two independent experiments. BrdU application was 1 hour before killing. *n* denotes the total number of individual sections counted. The average cell number counted on each section was 340. The small difference of wild-type and *Pax6^{Sey}/Pax6^{Sey}* LIs is statistically not significant (*t*-test).

Table 2. Quantification of cells migrating from EGL explants

Marker	Percentage of marker-positive cells	Total number of cells counted	Number of explants examined
D28K	<1	1215	10
Pax2	9	3931	5
GFAP	10	3715	11
Pax6	75	3237	11

Microexplants after 72 hours in culture were stained for markers of Purkinje cells (D28K), Golgi neurons (Pax2), for glial cells (GFAP) and for Pax6.

to become post-mitotic were assessed using the monoclonal antibody TuJ1 against neuron-specific β-tubulin (Lee et al., 1990), which specifically labels post-mitotic neurons. In wild-type EGL, TuJ1-positive cells are tightly localised exclusively in the premigratory zone (Fig. 4G). In contrast, in *Pax6^{Sey}/Pax6^{Sey}* cerebellum there are TuJ1-positive granule cells randomly scattered in the EGL, and no recognisable premigratory zone is formed (Fig. 4H). These results were confirmed by cumulative BrdU labelling. All proliferating cells were labelled at late E17 by a series of 6 BrdU injections over a 15 hour period. In wild-type EGL, analysed at E18.5, all cells of the germinal layer were BrdU+. BrdU− cells (which were therefore post-mitotic at the start of the experiment) were located only in the premigratory zone (Fig. 4I). In contrast, there were BrdU− cells located at random positions in the *Pax6^{Sey}/Pax6^{Sey}* EGL (Fig. 4J). *Pax6^{Sey}/Pax6^{Sey}* granule cells do reach post-mitotic (and therefore premigratory) status, but despite commitment to granule cell fate (see below), they are mal-positioned within the EGL. No abnormalities in the position or number of Purkinje cells, putative Golgi cells or deep cerebellar neurons is observed in mutant embryos.

Staining with antibodies against NCAM (not shown) or tau (Fig. 4K,L) reveals severely disorganised neuronal processes in the mutant cerebellar molecular layer: wild-type granule cell fibres align parallel to the pial surface while mutant fibres show no such regular orientation. Organisation of radial glia, revealed by staining with RC2 and 3CB2 (data not shown), appears normal in *Pax6^{Sey}/Pax6^{Sey}* cerebellum, apart from slight disturbance of glial fibres at the boundary EGL/molecular layer boundary.

Within limitations of the assay, there was no detectable difference in levels of cell death between mutant and wild-type EGL at E17.5; while at E18.5 an increase, from 1% to 3%, of TUNEL-positive cells was observed.

Marker profile of granule cells: a major alteration in Unc5h3 expression

Pax6 is expressed in wild-type granule cells from their formation onwards, highest levels being observed from days E17 to P2 (Figs 4D, 5A). Pax6 expression can be clearly observed by in situ hybridisation in wild-type and *Pax6^{Sey}/Pax6^{Sey}* EGL from E15.5 (Fig. 5A,B). Cell proliferation and differentiation continue in *Pax6^{Sey}/Pax6^{Sey}* cerebellum, despite some degree of disorganisation (see above and Fig. 4). It was of interest, therefore, to compare the marker profile of wild-type and *Pax6^{Sey}/Pax6^{Sey}* granule cells. EGL-expressed transcriptional regulators Math1, Zic1 and Zic2, as well as netrin receptors Dcc and Unc5h3 were examined. RNA in situ hybridisation reveals normal Math1, Zic1 and Zic2 expression in the *Pax6^{Sey}/Pax6^{Sey}* cerebellum (Fig. 5C,D; and data not shown). Spatiotemporal pattern and transcript levels are similar in wild-type and mutant EGL, suggesting that the initial determination of *Pax6^{Sey}/Pax6^{Sey}* rhombic lip cells to become granule cells is not disturbed. However, when the netrin receptors Dcc and Unc5h3 are studied, Dcc expression mirrors the Pax6, Math1/Zic1/Zic2 pattern (Fig. 5E,F), but Unc5h3 expression is absent in *Pax6^{Sey}/Pax6^{Sey}* EGL cells (compare Fig. 5G and 5H), although expression is completely normal in the neighbouring Purkinje cells, which are derived from a different lineage. Interestingly, parasagittal sections (Fig. 5A-F) show a small proportion of granule cells in *Pax6^{Sey}/Pax6^{Sey}* migrating ectopically in the direction of the inferior colliculus (Fig. 5B,D,F).

Disturbances in foliation and granule cell neurite extension in *Pax6^{Sey}/Pax6^{Sey}* cerebellum

Signals from cerebellar white matter contribute to positioning of fissures

Migration defects and/or signalling anomalies may constitute major underlying causes for the observed failure of normal foliation in *Pax6^{Sey}/Pax6^{Sey}* cerebellum. To explore possible signalling pathways, markers indicating possible pre-patterning of folia were identified. Antibodies against PSA-NCAM and Pax2 revealed expression patterns suggesting that fissure positions are determined before folia can be discerned. PSA-NCAM is expressed at the inner border of the EGL. Strongest expression is at positions where foliation is just beginning (Fig. 5I) and levels decrease after fissure formation is completed. At E18.5 PSA-NCAM staining in the *Pax6^{Sey}/Pax6^{Sey}* cerebellum resembles a foliated structure although no parallel EGL folding is seen (Fig. 5J). Pax2-positive neurons originate at the anterior base of the cerebellum and then migrate through the white matter toward the EGL. Coronal sections of E18.5 cerebellum reveal the Pax2-positive migration stream splitting caudally into several smaller streams, each pointing to a folial apex (Fig. 5K). Surprisingly, mutant cerebellum also shows a pattern of Pax2 expression resembling foliation (Fig. 5L), suggesting that foliation pre-patterning is undisturbed in *Pax6^{Sey}/Pax6^{Sey}* cerebellum.

BrdU labelling

TuJ1 labelling between E15.5 and E18.5 in cerebellar horizontal sections, suggested that more postmitotic granule cells are generated in lateral than medial EGL. A single dose of BrdU was applied at E15.5 and the results analysed at E18.5. Cells that go through no further division after BrdU

Table 3. Numbers of cells migrating early from mutant and wild-type EGL explants

	Percentage of explants with x number of cells migrating from explant				
	x<20	x=20-100	x>100	*n*	Exp.
wild-type	83	13	4	265	11
Pax6^{Sey}/Pax6^{Sey}	8	15	77	184	7

Cerebellar explants were cultured for 17 hours and then grouped in 3 categories by counting cells that had migrated away from the explant body. *n*, number of individual explants; Exp., number of independent experiments.

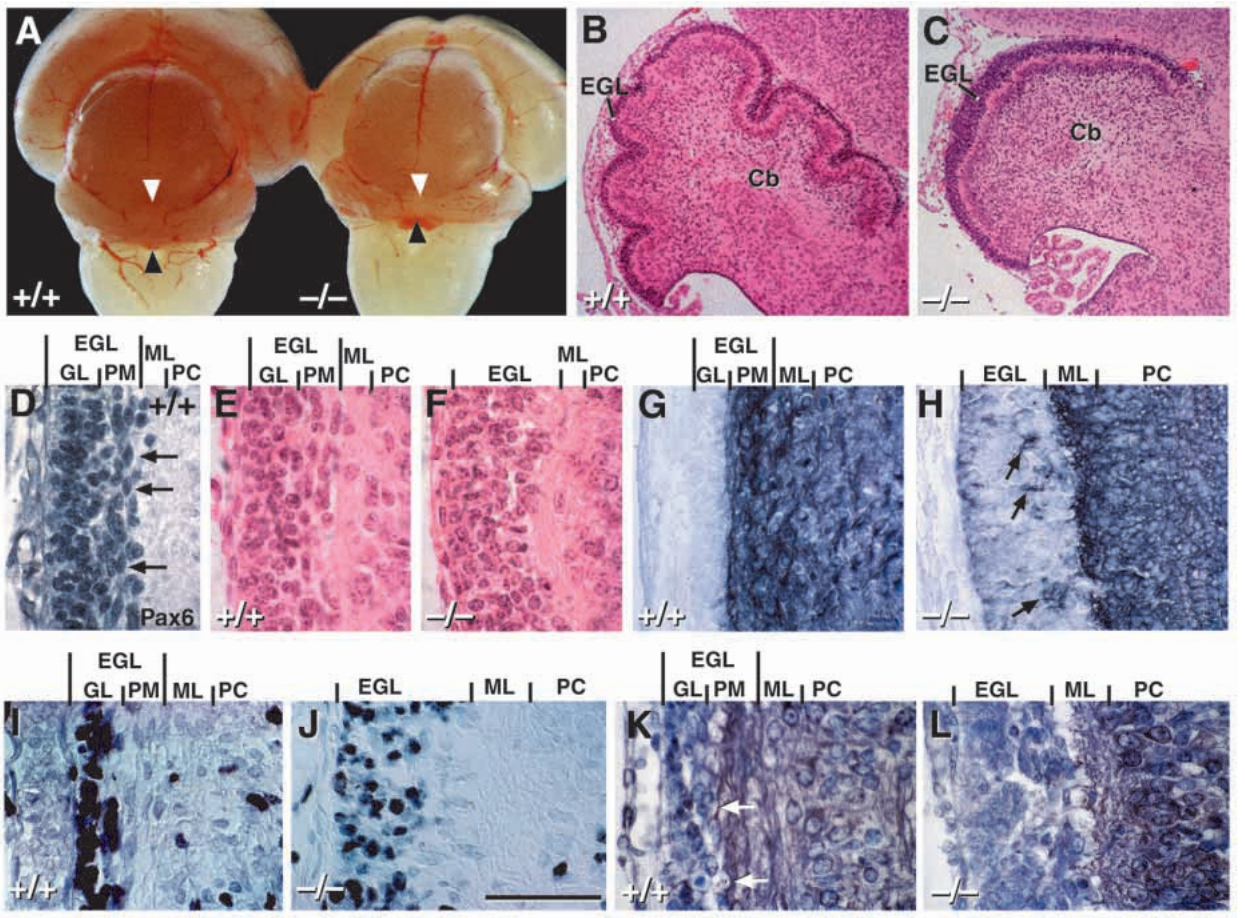

Fig. 4. Mutant cerebellar phenotype. (A) Wild-type (left) and *Pax6^{Sey}/Pax6^{Sey}* cerebella at E18.5. The lateral edges are much broader and the central vermal region is much narrower (arrowheads) in Pax6^{Sey}/Pax6^{Sey} cerebellum. (B) Wild-type and (C) *Pax6^{Sey}/Pax6^{Sey}* H+E stained E19.5 cerebellum. The *Pax6^{Sey}/Pax6^{Sey}* cerebellum has a thickened EGL and no fissures. (D-F) Transverse E18.5 sections through the cerebellar wild-type (D,E) and *Pax6^{Sey}/Pax6^{Sey}* (F) EGL. D is immuno-stained for Pax6; (E,F) are H+E stained: wild-type Pax6+ granule cell bodies in the premigratory zone are stretched parallel to the cerebellar surface (arrows in D). *Pax6^{Sey}/Pax6^{Sey}* granule cells are randomly orientated and no premigratory zone can be distinguished. (G-L) Transverse sections through the E18.5 wild-type (G,I,K) and mutant (H,J,L) cerebellum, stained with TuJ1 (G,H), anti-BrdU (I,J) and anti-tau (K,L) antibodies. Postmitotic TuJ1-positive granule cells in the wild-type EGL (G) are located in the premigratory zone and orientated parallel to the pial surface. In *Pax6^{Sey}/Pax6^{Sey}* EGL (H), TuJ1-positive cells are scattered in the EGL and fail to reorient (arrows). (I,J) BrdU-stained transverse sections of embryos that received six serial injections of BrdU between E17.5 and E18.5. In wild-type EGL (I) all cells in the germinal layer are BrdU+ and the majority of cells in the premigratory layer are BrdU–, indicating that these were postmitotic at E17.5. In the mutant (J), BrdU– cells are scattered throughout the EGL. (K,L) tau antibody staining for neuronal fibers show that wild-type cerebellar neuronal fibers align parallel to the pial surface (white arrows in K), whilst mutant fibers (L) show no consistent orientation. CP, cerebellar primordium; Cb, cerebellum; EGL, external granule cell layer; GL, germinal layer; ML, molecular layer; PM, premigratory zone; PC, Purkinje cell layer; +/+ and –/– indicate wild-type and *Pax6^{Sey}/Pax6^{Sey}* embryos respectively. Scale bar, 2.2 μm in A; 400 μm in B, C; 40 μm in D,E,F,G,H; 60 μm in I,J,K,L.

application remain strongly BrdU+, but those that continue to divide further become weakly labelled or negative. Labelling indices (LI = BrdU positive/total cells) were assessed at E18.5: laterally at 1 mm, and medially at 0.2 mm, from the midline. In wild-type the lateral and medial figures were 42.4 (±2.9)% (n=3) and 46.2 (±3.1)% (n=3), respectively, while in *Pax6^{Sey}/Pax6^{Sey}*, the comparable figures were 50.2 (±2.5)% (n=3) and 32.8 (±2.6)% (n=3), showing a significant reduction in medial labelling. At the same time, the lateral to medial distribution of TuJ1+ postmitotic cells was almost even in wild-type cerebellum, whereas in the mutant postmitotic cells accumulate laterally, with a virtual absence of TuJ1-labelled cells medially (data not shown).

Cerebellar explant cultures to study neurite extension

Immunostaining with tau, NCAM or TuJ1 antibodies suggests severe disruption of neuronal fibre formation in the postmitotic granule cell region of *Pax6^{Sey}/Pax6^{Sey}* mutants. To examine this further, wild-type and mutant EGL microexplant cultures were set up, as described (Nakatsuji and Nagata, 1989). 75% of emigrating cells from wild-type controls are Pax6+ (Table 2). By 17 hours short neuronal processes have extended from wild-type fragments, but very few cell bodies have migrated out. In contrast many densely packed mutant *Pax6*-expressing cells have migrated away from comparable *Pax6^{Sey}/Pax6^{Sey}* explants (Table 3). After 40 hours multiple cell bodies can be seen migrating along each extending process in wild-type explants (Fig. 6A) while in *Pax6^{Sey}/Pax6^{Sey}* cultures without leading

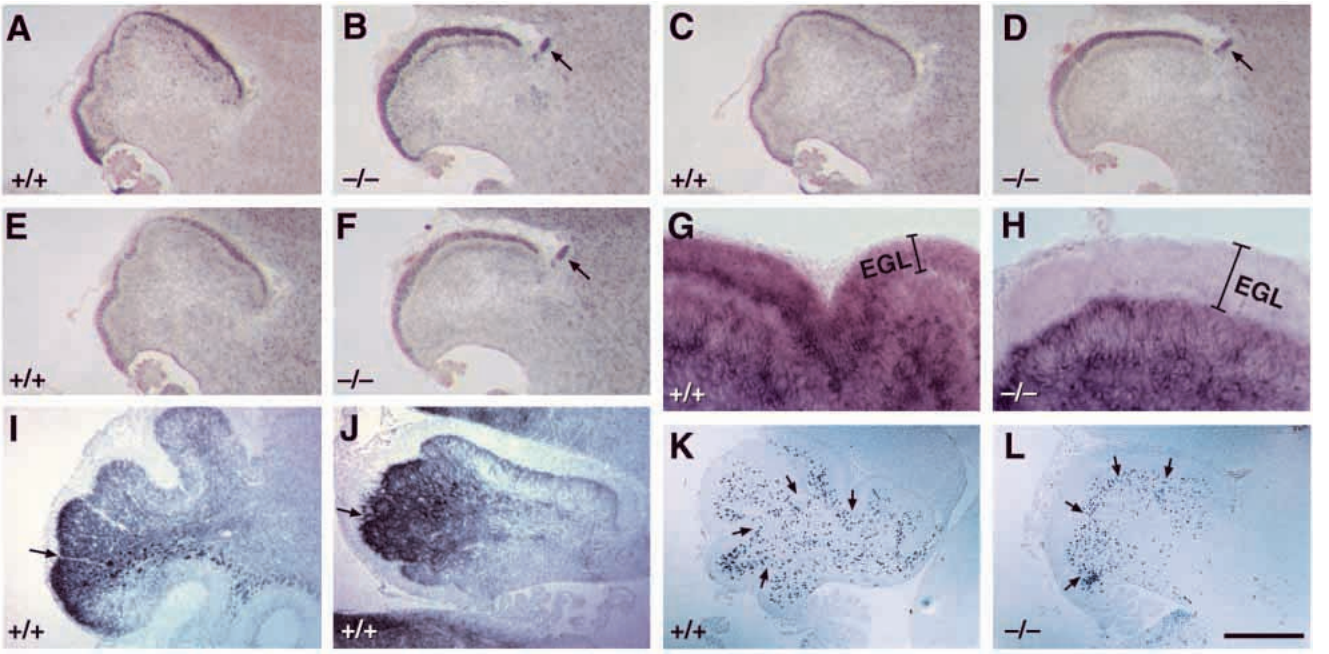

Fig. 5. Cerebellar marker expression and foliation signals. (A-F) RNA in situ hybridisation of parasagittal sections through wild-type (A,C,E) and mutant (B,D,F) E17.5 cerebellum for Pax6 (A,B), Math1 (C,D) and Dcc (E,F). Math1 and Dcc are both expressed in the wild-type and the *Pax6^{Sey}/Pax6^{Sey}* EGL, as is the mutant Pax6 mRNA. Note ectopic granule cells at the inferior colliculus in mutant embryos (arrows in B,D,F). (G,H) Vibratome sections of wild-type (G) and mutant (H) cerebellum showing Unc5h3 expression by whole mount in situ hybridisation. Unc5h3 is absent from *Pax6^{Sey}/Pax6^{Sey}* granule cells, but continues to be expressed in Purkinje cells. (I) Wild-type and (J) *Pax6^{Sey}/Pax6^{Sey}* parasagittal sections of E18.5 cerebellum showing strong immunohistochemical PSA-NCAM expression in white matter preceding fissure formation in wild-type EGL (arrow in I); a very similar pattern is seen in the mutant (arrow in J). (K) Wild-type and (L) *Pax6^{Sey}/Pax6^{Sey}* parasagittal sections of E18.5 cerebellum stained with anti-Pax2 antibody. In wild-type cerebellum Pax2+ neurons migrate from the cerebellar neuroepithelium toward the tips of the folia. In mutant cerebellum (L) very similar expression and migration patterns are seen for Pax2+ neurons, resembling those associated with normal foliation. Arrows indicate positions of the four primary fissures. EGL, external granule cell layer; PC, Purkinje cell layer; +/+ and –/– indicate wild-type and *Pax6^{Sey}/Pax6^{Sey}* embryos respectively. Scale bar, 350 μm in A-F; 50 μm in G,H; 300 μm in I-L.

processes disorganised cell migration occurs (Fig. 6B). Differences are reinforced after 72 hours in culture (Fig. 6C,D,E,F). Emigrating cells from wild-type and mutant explants are Pax6-expressing, as visualised by immunofluorescence (Fig. 6C,E) and RNA in situ hybridisation (Fig. 6D inset) respectively; the extending fibres are NCAM+. After 80 hours in culture these neuronal processes can be several hundred microns long in wild-type explants. Neuronal proteins NCAM, tau, GAP-43 (Fig. 6D,G and data not shown) are also synthesised by *Pax6^{Sey}/Pax6^{Sey}* granule cells but remain localised around the cell body rather than reorganising into

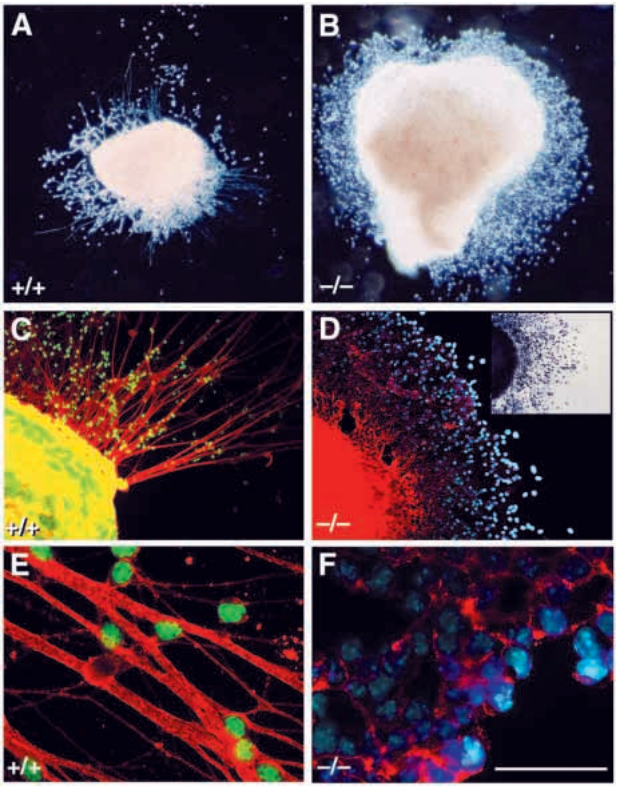

Fig. 6. Cerebellar microexplant cultures. (A,B) Phase contrast images of wild-type (A) and mutant (B) explants after 40 hours in culture. *Pax6^{Sey}/Pax6^{Sey}* cells grow out as a dense monolayer with almost no intercellular spaces. (C-F) Explants cultured for 72 hours. (C,E) Wild-type cultures immunostained for Pax6 (green) and NCAM (red) expression. Wild-type cells form long neuronal processes which direct migration of succeeding cells. (D,F) *Pax6^{Sey}/Pax6^{Sey}* cultures immunostained for NCAM (red) expression and counterstained with DAPI (blue) as antibody staining in mutant nuclei is very weak. *Pax6^{Sey}/Pax6^{Sey}* cells lack neuronal processes so that NCAM is tightly localised around the nuclei. The inset in D shows a mutant explant with Pax6^{Sey} mRNA expression revealed by in situ hybridisation. EGL, external granule cell layer; ML, molecular layer; PC, Purkinje cell layer; ps, pial surface +/+ and –/– indicate wild-type and *Pax6^{Sey}/Pax6^{Sey}* embryos respectively. Scale bar, 400 μm in A,B; 250 μm in C,D; 40 μm in E,F.

elongated migration-promoting processes. Mutant neurons are more tightly packed and more adherent to the substratum.

DISCUSSION

Examination of the developing cerebellar system in normal and Pax6-null mouse embryos, has revealed abnormalities in structures derived from both caudal and rostral rhombic lip. Development of three of the five precerebellar nuclei is severely disrupted, although cell proliferation is unaltered. In the cerebellum, the Pax6-expressing external granule cell layer is disorganised and broadened as foliation fails to take place, while proliferative capacity and foliation signals appear undisturbed. Several granule cell markers are expressed normally, but the netrin receptor Unc5h3 is completely absent in the mutant EGL, suggesting a loss of responsiveness to some essential signalling cues. Cerebellar explant cultures illustrate the altered capacity of mutant tissue to extend cellular processes, required for the normal emigration of cell bodies.

Role of Pax6 in CNS development

Pax6 appears to fulfil different roles in development of the forebrain and cerebellum. In the telencephalon, the Pax6+ ventricular layer gives rise to virtually all cortical cells including glia and neurons, whereas in cerebellum Pax6+ rhombic lip precursors give rise solely to granule cells (Alder et al., 1996): other cell types (Purkinje cells, interneurons and radial glia) are of Pax6− neuroepithelial origin (Altman and Bayer, 1997). In *Pax6^{Sey}/Pax6^{Sey}* forebrain proliferation defects were reported (Warren and Price, 1997; Götz et al., 1998) which are not observed in rhombic lip-derived structures. In the telencephalon, Pax6 controls the differentiation of radial glia (Götz et al., 1998), whereas, in *Pax6^{Sey}/Pax6^{Sey}* cerebellum, granule cell behaviour is altered. In addition, marked morphological differences exist between cortical and cerebellar radial glia: the former are bipolar, the latter monopolar (Misson et al., 1988). Even among rhombic lip derivatives, Pax6 appears to function upstream of different genetic pathways: whilst Unc5h3 is still expressed in mutant pontine and RT remnants, it is completely absent in the mutant EGL, suggesting a loss of responsiveness to some essential signalling cues.

Role of *Pax6* in generation of precerebellar nuclei

Formation of the precerebellar nuclei from the caudal rhombic lip-derived pcn, is an intriguing example of how a single germinal zone can give rise to several remotely dispersed neuronal sub-populations (Altman and Bayer, 1987). Once the lengthy migrations to distant target sites are completed, each of these nuclei projects back to the cerebellum (Altman and Bayer, 1987). The earliest migration to the inferior olive, via the circumferential intramural path (Altman and Bayer, 1987), involves Pax6− cells whose passage is unaltered in *Pax6^{Sey}/Pax6^{Sey}* mice. In contrast, the Pax6+ pes and its targets, the external cuneate and lateral reticular nuclei, are completely disorganised in *Pax6^{Sey}/Pax6^{Sey}* mice (D. E. et al., unpublished data). The aes is a dual migration stream, conveying cells to the strongly Pax6+ pontine and to the weakly Pax6+ reticulotegmental nuclei. Functional Pax6 expression is required for normal generation of pontine neurons: by E18.5 the cell numbers in the mutant pons are reduced to 10% of that in wild type. Possible explanations for the presence of the pontine remnant are: (a) a proportion of the pontine cells are Pax6-independent; (b) cells observed in the *Pax6^{Sey}/Pax6^{Sey}* pontine nuclei at E18.5 are in transit on their way to the reticulotegmental nucleus (not all RT cells have reached their target by E18.5; D. E., unpublished data); or (c) the predetermined aes pathway (see PSA-NCAM data Fig. 2F,H) is used illegitimately by a few pontine cells which are carried along with the migration-competent reticulotegmental cells. Resolution of these possibilities requires identification of marker(s) capable of distinguishing pontine and reticulotegmental neurons.

In contrast, careful examination shows that aes cells destined for the reticulotegmental nucleus, which migrate through the pontine nuclei and the cortico-spinal tract, are present. This migration is not disturbed in *Pax6^{Sey}/Pax6^{Sey}* embryos (Fig. 3E,F,L,M) suggesting a redundant role for Pax6 in these cells. Redundancy in Pax gene function has been noted previously: for Pax3/Pax7 in generation of commissural neurons (Mansouri and Gruss, 1998), and for Pax2/Pax5 in cerebellar development (Schwarz et al., 1997; Urbanek et al., 1997). A similar mechanism may be found for Pax6, although use of a pan-Pax-specific antibody has not revealed expression of any other Pax gene (D. E., unpublished data).

Wild-type migrating precerebellar neurons express the netrin receptor Dcc but switch to Unc5h3 as they arrive at their target site, perhaps suggesting tight control of normal cell movement through netrin guidance. In *Pax6^{Sey}/Pax6^{Sey}* embryos, Dcc expression in the aes is greatly reduced (Fig. 3K) while expression of PSA-NCAM, another guidance molecule, is unaltered (Fig. 2F,H). Unc5h3 expression appears to be maintained in cells that manage to reach the reticulotegmental or pontine nuclei by E18.5 (Fig. 3M). Thus some components of the migration pathway are specified independently of Pax6 function. Interestingly, loss of pontine nuclei has only been described previously in *Ntn1* and *Dcc* knockout mice (Fazeli et al., 1997; Serafini et al., 1996), but the fate of Pax6+ pcn and aes cells in these mutants has not been reported. It will be important to determine whether such cells are generated and end up in ectopic sites.

The primary role of Pax6 in development of the precerebellar system is unclear. Pax6 is highly expressed in precerebellar precursor cells at the pcn and subsequently during their active migration, but its expression is switched off once the target site is reached. Loss of precerebellar nuclei in *Pax6^{Sey}/Pax6^{Sey}* embryos suggests that Pax6 is involved either in cell fate determination and signalling, or in the processes of migration. Our results favour the second option because, (i) BrdU labelling suggests that *Pax6^{Sey}/Pax6^{Sey}* precerebellar cells are generated at a normal rate, (ii) cumulative labelling reveals no alternative ectopic target sites in the hindbrain, and (iii) enlargement of the E16.5 *Pax6^{Sey}/Pax6^{Sey}* pcn (Fig. 3G,H) suggests that the neurons are generated, but fail to migrate appropriately. The predominantly normal pattern of cell marker expression in the remaining pcn-derived cells suggests no radical alteration in cell fate determination. It is interesting to note that none of the migration anomalies observed in the *Pax6^{Sey}/Pax6^{Sey}* precerebellar system involve movement along radial glial fibres.

Pax6 in cerebellar development, granule cell differentiation and migration

The most striking alteration of cerebellar development observed in *Pax6^{Sey}/Pax6^{Sey}* mice is the lack of foliation. The nature of this defect remains unclear. Some foliation pre-patterning can be

observed in *Pax6^{Sey}/Pax6^{Sey}* cerebellar medulla, as illustrated by the PSA-NCAM and Pax2 expression domains (Fig. 5I-L), but presumably the *Pax6^{Sey}/Pax6^{Sey}* EGL cells are unable to respond appropriately to this. Nonetheless, proliferative cues from the Purkinje cells to granule cells (Wechsler-Reya and Scott, 1999) must be functional since proliferation is unaltered. Moreover disturbances are seen in the correct sorting and premigratory reorientation of post-mitotic cells in the mutant EGL. Regular alignment of tau-protein-expressing fibres is also disturbed. These aberrations may reflect a role for Pax6 in neurite extension. Intriguingly the *Pax6^{Sey}/Pax6^{Sey}* granule cells are incompletely specified: the netrin guidance receptor Unc5h3 is completely absent although other granule cell markers (Math1, Zic1, Zic2 and Dcc) appear to be expressed normally (Fig. 5A-F and data not shown). However, in the mutant, Unc5h3 is present normally in adjacent Purkinje cells (Fig. 5G,H), which are derived from Pax6– neuroepithelium. Unc5h3 therefore acts directly or indirectly downstream of Pax6 in the EGL. Interestingly, parasagittal sections of E17.5 *Pax6^{Sey}/Pax6^{Sey}* cerebellum reveal ectopic extensions of EGL cells towards the region of the inferior colliculus. Although Unc5h3^{rcm} homozygous mutant mice have a similar group of ectopic granule cells which appear to be migrating towards the inferior colliculus (Ackerman et al., 1997; Przyborski et al., 1998), neither fissure formation nor neurite extension seem to be affected in these mice. Therefore, the loss of Unc5h3 expression in granule cells cannot, by itself, account for all the observed *Pax6^{Sey}/Pax6^{Sey}* cerebellar defects.

EGL explant analysis (Fig. 6) also suggests that correct neurite extension is a pre-requisite for ordered emigration of nuclei (75% of which express Pax6) from the EGL. Migration failure from *Pax6^{Sey}/Pax6^{Sey}* explants is accompanied by increased cellular adherence to the substratum.

Cell counting and BrdU labelling experiments support the suggestion that the Pax6-null cerebellar phenotype, including foliation failure, may be associated with aberrant cell movement. Cell proliferation was unaltered in all regions of the mutant cerebellum (Table 1), but following BrdU labelling at E15.5 and analysis at E18.5, an increase in LI and an accumulation of postmitotic cells was observed laterally. The altered gross shape of the cerebellum is also consistent with reduced lateral to medial cell movement. In chick, Ryder and Cepko (1994) observed transverse granule cell migration predominantly in the lateral to medial direction and suggested that this movement might be involved in cerebellar fissure formation.

Comparative analysis of cerebellar system development in normal and mutant mice offers a potent opportunity for further dissection of the role of Pax6 and its direct and indirect downstream targets, which may well be different in each Pax6-expressing tissue. Classification of more cell-specific markers to differentiate between the different pcn derivatives and granule cells, as well as identification of Pax6 target genes, will provide molecular insight into how different mutant phenotypes are produced.

Hypothesis

A possible unifying role for *Pax6* may be in the control of interkinetic nuclear migration (Sauer, 1935), which was shown to be altered in *Pax6^{Sey}/Pax6^{Sey}* forebrain (Götz et al., 1998). Cortical cells derived from ventricular germinal zones undergo this type of fluctuating movement as an essential component of the cell division process at the spatially limited columnar ventricular surface (Choi, 1991). Impairment of this process would lead to altered proliferation rates. Pax6-expressing hindbrain neurons, however, are generated at the pcn and the EGL with virtually no spatial limitation. These germinal zones are not organised as columnar epithelia and the typical ‘up-and-down’ migration of nuclei has not been observed during cell division (D. E., unpublished observations). Proliferative activity would therefore remain undisturbed in the *Pax6^{Sey}/Pax6^{Sey}* pcn and EGL. Long distance migration of granule cells and of neurons derived from the pcn do, however, involve a similar process: neurite extension in the direction of future movement and subsequent perikaryal translocation of the nucleus (Book et al., 1991; Liesi, 1992). Disturbance of this process in postmitotic granule cells may underlie the failure to form a distinct pre-migratory layer, and the altered explant culture behaviour.

Comparative analysis of cerebellar system development in normal and mutant mice, offers a potent opportunity for further dissection of the role of *Pax6* and its direct and indirect downstream targets, which may well be different in each Pax6-expressing tissue. Future identification of Pax6 target genes will provide molecular insight into how different mutant phenotypes are produced.

We thank G. Rougon, M. Dressler and A. Frankfurter for gifts of antibodies and M. Tessier-Lavigne, J. Aruga, H. Y. Zhogby and S. Ackerman for probes. We are grateful to the staff of the BRF, Western General Hospital for technical assistance and to Norman Davidson and Douglas Stuart for photographic expertise. V. vH. was an HHMI International Scholar. D. E. was supported by a Wellcome Trust International Travelling Fellowship, the MRC and the Max Planck Society. P. R. was an MRC Clinical Training Fellow. The authors wish to thank the anonymous referee whose suggestions helped to improve this manuscript.

REFERENCES

Ackerman, S. L., Kozak, L. P., Przyborski, S. A., Rund, L. A., Boyer, B. B. and Knowles, B. B. (1997). The mouse rostral cerebellar malformation gene encodes an UNC-5-like protein. *Nature* **386**, 838-842.

Alder, J., Cho, N. K. and Hatten, M. E. (1996). Embryonic precursor cells from the rhombic lip are specified to a cerebellar granule neuron identity. *Neuron* **17**, 389-399.

Altman, J. and Bayer, S. A. (1987). Development of the precerebellar nuclei in the rat: I.-IV. *J. Comp. Neurol.* **257**, 477-552.

Altman, J. and Bayer, S. A. (1997). Development of the cerebellar system in relation to its evolution, structure, and functions. Boca Raton: CRC Press.

Aruga, J., Minowa, O., Yaginuma, H., Kuno, J., Nagai, T., Noda, T. and Mikoshiba, K. (1998). Mouse Zic1 is involved in cerebellar development. *J. Neurosci.* **18**, 284-93.

Ben-Arie, N., Bellen, H. J., Armstrong, D. L., McCall, A. E., Gordadze, P. R., Guo, Q., Matzuk, M. M. and Zoghbi, H. Y. (1997). Math1 is essential for genesis of cerebellar granule neurons. *Nature* **390**, 169-172.

Book, K. J., Howard, R. and Morest, D. K. (1991). Direct observation in vitro of how neuroblasts migrate: medulla and cochleovestibular ganglion of the chick embryo. *Exp. Neurol.* **111**, 228-243.

Brown, S. A., Warburton, D., Brown, L. Y., Yu, C. Y., Roeder, E. R., Stengel-Rutkowski, S., Hennekam, R. C. and Muenke, M. (1998). Holoprosencephaly due to mutations in ZIC2, a homologue of Drosophila odd-paired. *Nat. Genet.* **20**, 180-183.

Callaerts, P., Halder, G. and Gehring, W. J. (1997). PAX-6 in development and evolution. *Annu. Rev. Neurosci.* **20**, 483-532.

Caric, D., Gooday, D., Hill, R. E., McConnell, S. K. and Price, D. J. (1997). Determination of the migratory capacity of embryonic cortical cells lacking the transcription factor Pax-6. *Development* **124**, 5087-5096.

Chisholm, A. D. and Horvitz, H. R. (1995). Patterning of the Caenorhabditis elegans head region by the Pax-6 family member vab-3. *Nature* **377**, 52-55.

Choi, B. H. (1991). Effects of methylmercury on neuroepithelial germinal cells

in the developing telencephalic vesicles of mice. *Acta Neuropathologica* **81**, 359.

Dressler, G. R. and Douglass, E. C. (1992). Pax-2 is a DNA-binding protein expressed in embryonic kidney and Wilms tumor. *Proc. Natl. Acad. Sci. USA* **89**, 1179-83.

Ericson, J., Rashbass, P., Schedl, A., Brenner-Morton, S., Kawakami, A., van Heyningen, V., Jessell, T. M. and Briscoe, J. (1997). Pax6 controls progenitor cell identity and neuronal fate in response to graded Shh signaling. *Cell* **90**, 169-180.

Essik, C. R. (1912). The development of the nuclei pontis and the nucleus arcuatus in man. *Am. J. Anat.* **13**, 25-54.

Fazeli, A., Dickinson, S. L., Hermiston, M. L., Tighe, R. V., Steen, R. G., Small, C. G., Stoeckli, E. T., Keino-Masu, K., Masu, M., Rayburn, H. et al. (1997). Phenotype of mice lacking functional Deleted in colorectal cancer (Dcc) gene. *Nature* **386**, 796-804.

Götz, M., Stoykova, A. and Gruss, P. (1998). Pax6 controls radial glia differentiation in the cerebral cortex. *Neuron* **21**, 1031.

Grindley, J. C., Davidson, D. R. and Hill, R. E. (1995). The role of Pax-6 in eye and nasal development. *Development* **121**, 1433-1442.

Grindley, J. C., Hargett, L. K., Hill, R. E., Ross, A. and Hogan, B. L. (1997). Disruption of PAX6 function in mice homozygous for the *Pax6$^{Sey-1Neu}$* mutation produces abnormalities in the early development and regionalization of the diencephalon. *Mech. Dev.* **64**, 111-126.

Halder, G., Callaerts, P. and Gehring, W. J. (1995). Induction of ectopic eyes by targeted expression of the eyeless gene in Drosophila. *Science* **267**, 1788-1792.

Hallonet, M. E., Teillet, M. A. and Le Douarin, N. M. (1990). A new approach to the development of the cerebellum provided by the quail-chick marker system. *Development* **108**, 19-31.

Hanson, I. and van Heyningen, V. (1995). Pax6: more than meets the eye. *Trends Genet.* **11**, 268-272.

Hatten, M. E. and Heintz, N. (1995). Mechanisms of neural patterning and specification in the developing cerebellum. *Annu. Rev. Neurosci.* **18**, 385-408.

Hill, R. E., Favor, J., Hogan, B. L., Ton, C. C., Saunders, G. F., Hanson, I. M., Prosser, J., Jordan, T., Hastie, N. D. and van Heyningen, V. (1991). Mouse small eye results from mutations in a paired-like homeobox-containing gene [published erratum appears in *Nature* 1992 Feb 20;**355**(6362):750]. *Nature* **354**, 522-525.

His, W. (1891). Die Entwicklung des menschlichen Rautenhirns vom Ende des ersten bis zum Beginn des dritten Monats. I. Verlängertes Mark. *Abh. kö. sächs. Ges. d. Wis., Mat. Phys. Kl.* **29**, 1-47.

Keino-Masu, K., Masu, M., Hinck, L., Leonardo, E. D., Chan, S. S., Culotti, J. G. and Tessier-Lavigne, M. (1996). Deleted in Colorectal Cancer (Dcc) encodes a netrin receptor. *Cell* **87**, 175-85.

Kennedy, T. E., Serafini, T., de la Torre, J. R. and Tessier-Lavigne, M. (1994). Netrins are diffusible chemotropic factors for commissural axons in the embryonic spinal cord. *Cell* **78**, 425-435.

Köhler, G. and Milstein, C. (1975). Continuous cultures of fused cells secreting antibody of predefined specificity. *Nature* **256**, 495-497.

Larsson, S. H., Charlieu, J. P., Miyagawa, K., Engelkamp, D., Rassoulzadegan, M., Ross, A., Cuzin, F., van Heyningen, V. and Hastie, N. D. (1995). Subnuclear localization of WT1 in splicing or transcription factor domains is regulated by alternative splicing. *Cell* **81**, 391-401.

Lee, M. K., Tuttle, J. B., Rebhun, L. I., Cleveland, D. W. and Frankfurter, A. (1990). The expression and posttranslational modification of a neuron-specific beta-tubulin isotype during chick embryogenesis. *Cell Motil. Cytoskel.* **17**, 118-132.

Liesi, P. (1992). Neuronal migration on laminin involves neuronal contact formation followed by nuclear movement inside a preformed process. *Exp. Neurol.* **117**, 103-113.

Mansouri, A. and Gruss, P. (1998). Pax3 and Pax7 are expressed in commissural neurons and restrict ventral neuronal identity in the spinal cord. *Mech. Dev.* **78**, 171.

Marín, F. and Puelles, L. (1995). Morphological fate of rhombomeres in quail/chick chimeras: a segmental analysis of hindbrain nuclei. *Eur. J. Neurosci.* **7**, 1714-38.

Mastick, G. S., Davis, N. M., Andrew, G. L. and Easter, S. S., Jr. (1997). Pax-6 functions in boundary formation and axon guidance in the embryonic mouse forebrain. *Development* **124**, 1985-1997.

Miale, I. and Sidman, R. L. (1961). An autoradiographic analysis of histogenesis in the mouse cerebellum. *Exp. Neurol.* **4**, 277-296.

Misson, J. P., Edwards, M. A., Yamamoto, M. and Caviness, V. S., Jr. (1988). Identification of radial glial cells within the developing murine central nervous system: studies based upon a new immunohistochemical marker. *Dev. Brain Res.* **44**, 95-108.

Nakatsuji, N. and Nagata, I. (1989). Paradoxical perpendicular contact guidance displayed by mouse cerebellar granule cell neurons in vitro. *Development* **106**, 441-447.

Osumi, N., Hirota, A., Ohuchi, H., Nakafuku, M., Iimura, T., Kuratani, S., Fujiwara, M., Noji, S. and Eto, K. (1997). Pax-6 is involved in the specification of hindbrain motor neuron subtype. *Development* **124**, 2961-2972.

Pierce, E. T. (1966). Histogenesis of the nuclei griseum pontis, corporis pontobulbaris and reticularis tegmenti pontis (Bechterew) in the mouse. An autoradiographic study. *J. Comp. Neurol.* **126**, 219-254.

Prada, F. A., Dorado, M. E., Quesada, A., Prada, C., Schwarz, U. and de la Rosa, E. J. (1995). Early expression of a novel radial glia antigen in the chick embryo. *Glia* **15**, 389-400.

Przyborski, S. A., Knowles, B. B. and Ackerman, S. L. (1998). Embryonic phenotype of Unc5h3 mutant mice suggests chemorepulsion during the formation of the rostral cerebellar boundary. *Development* **125**, 41-50.

Rakic, P. (1990). Principles of neural cell migration. *Experientia* **46**, 882-891.

Ramón y Cajal, S. (1995). *Histology of the Nervous System of Man and Vetebrates.* New York: Oxford University Press.

Roberts, R. C. (1967). Small-eyes, a new dominant mutation in the mouse. *Genetic Re. Camb.* **9**, 121-122.

Rougon, G., Dubois, C., Buckley, N., Magnani, J. L. and Zollinger, W. (1986). A monoclonal antibody against meningococcus group B polysaccharides distinguishes embryonic from adult N-CAM. *J. Cell Biol.* **103**, 2429-2437.

Ryder, E. F. and Cepko, C. L. (1994). Migration patterns of clonally related granule cells and their progenitors in the developing chick cerebellum. *Neuron* **12**, 1011-1028.

Sauer, F. C. (1935). Mitosis in the neural tube. *J. Comp. Neurol.* **62**, 377-405.

Schmahl, W., Knoedlseder, M., Favor, J. and Davidson, D. (1993). Defects of neuronal migration and the pathogenesis of cortical malformations are associated with Small eye (Sey) in the mouse, a point mutation at the Pax-6-locus. *Acta Neuropath.* **86**, 126-135.

Schwarz, M., Alvarezbolado, G., Urbanek, P., Busslinger, M. and Gruss, P. (1997). Conserved biological function between Pax-2 and Pax-5 in midbrain and cerebellum development – evidence from targeted mutations. *Proc. Natl. Acad. Sci. USA* **94**, 14518-14523.

Serafini, T., Colamarino, S. A., Leonardo, E. D., Wang, H., Beddington, R., Skarnes, W. C. and Tessier-Lavigne, M. (1996). Netrin-1 is required for commissural axon guidance in the developing vertebrate nervous system. *Cell* **87**, 1001-14.

Stoykova, A., Fritsch, R., Walther, C. and Gruss, P. (1996). Forebrain patterning defects in Small eye mutant mice. *Development* **122**, 3453-3465.

Stoykova, A. and Gruss, P. (1994). Roles of Pax-genes in developing and adult brain as suggested by expression patterns. *J. Neurosci.* **14**, 1395-1412.

Strähle, U., Blader, P., Adam, J. and Ingham, P. W. (1994). A simple and efficient procedure for non-isotopic in situ hybridization to sectioned material. *Trends Genet.* **10**, 75-76.

Sun, T., Pringle, N. P., Hardy, A. P., Richardson, W. D. and Smith, H. K. (1998). Pax6 influences the time and site of origin of glial precursors in the ventral neural tube. *Mol. Cell. Neurosci.* **12**, 228.

Takahashi, T., Nowakowski, R. S. and Caviness, V. S., Jr. (1992). BUdR as an S-phase marker for quantitative studies of cytokinetic behaviour in the murine cerebral ventricular zone. *J. Neurocyt.* **21**, 185-197.

Urbanek, P., Fetka, I., Meisler, M. H. and Busslinger, M. (1997). Cooperation of Pax2 and Pax5 in midbrain and cerebellum development. *Proc. Natl. Acad. Sci. USA* **94**, 5703-5708.

Walther, C. and Gruss, P. (1991). *Pax-6*, a murine paired box gene, is expressed in the developing CNS. *Development* **113**, 1435-1449.

Warren, N. and Price, D. J. (1997). Roles of Pax-6 in murine diencephalic development. *Development* **124**, 1573-1582.

Wechsler-Reya, R. J., and Scott, M. P. (1999). Control of neuronal precursor proliferation in the cerebellum by sonic hedgehog. *Neuron* **22** 103-114.

Zhang, L. and Goldman, J. E. (1996). Developmental fates and migratory pathways of dividing progenitors in the postnatal rat cerebellum. *J. Comp. Neurol.* **370**, 536-550.

Zhang, Y. and Emmons, S. W. (1995). Specification of sense-organ identity by a Caenorhabditis elegans Pax-6 homologue. *Nature* **377**, 55-59.